0026-895X/96/040900-12$3.00/0

MOLECULAR PHARMACOLOGY, 50:900–911 (1996).

DNA-Damaging Agents Induce Both p53-Dependent and p53-Independent Apoptosis in Immature Thymocytes

MARION MACFARLANE, NEIL A. JONES, CAROLINE DIVE, and GERALD M. COHEN

MRC Toxicology Unit, University of Leicester, Leicester LE1 9HN, UK (M.M., G.M.C.), and CRC Molecular and Cellular Pharmacology Group, School of Biological Sciences, University of Manchester, Manchester M13 9PT, UK (N.A.J., C.D.)

Received November 20, 1995; Accepted June 27, 1996

SUMMARY

Apoptosis in the immature thymus can be induced by both p53-dependent and -independent pathways, the former being activated by exposure to DNA-damaging agents and the latter being induced by glucocorticoids [*Nature (Lond.)* **362**:847–849; *Nature (Lond.)* **362**:849–852 (1993)]. We report that the DNA-damaging agents etoposide and γ-radiation induced similar levels of apoptosis in both proliferatively enriched and quiescent immature rat thymocytes, as assessed by flow cytometry and the formation of both kilobase-pair and 180-bp integer fragments of DNA. However, a marked stabilization of p53 occurred exclusively in the proliferatively enriched population, which was also enriched for immature $CD4^-CD8^-$ and mature $CD4^+CD8^-/CD4^-CD8^+$ cells. In contrast, DNA damage-induced apoptosis in quiescent mature peripheral T cells was associated with an accumulation of p53. Our studies suggest that stabilization of p53 in thymocytes in response to DNA damage may be developmentally regulated. In immature thymocytes obtained from p53-null mice, DNA-damaging agents induced apoptosis at significantly lower levels and at later times than that seen in cells from p53 wild-type animals. These data support the hypothesis that DNA-damaging agents induce apoptosis primarily via a p53-dependent pathway in immature thymocytes as previously reported. We report here that DNA damage can also induce apoptosis by a p53-independent pathway in a particular subpopulation of immature thymocytes.

Apoptosis is a specific mode of cell death that is characterized by a well-defined pattern of morphological, biochemical, and molecular changes (1–3). Apoptosis can be triggered by diverse factors in the cell environment, and it plays a key role in normal cell turnover, tissue and organ development during embryogenesis, and immune and toxic cell killing (4–6).

Death of immature thymocytes triggered by corticosteroid hormones or other agents is generally considered to be a classic model of apoptosis. In this system, apoptosis is best characterized morphologically by chromatin condensation and cell shrinkage (4, 7). It has also been characterized biochemically by the cleavage of DNA into nucleosomal size fragments of 180–200 bp or multiples thereof, which are detected by gel electrophoresis as a DNA ladder (3, 6, 8). More recently, we and others have shown that DNA is initially cleaved to 200–300- and 30–50-kbp fragments (9–12), which are then further degraded to produce oligonucleosomes and the typical DNA ladder pattern. In thymocytes, apoptosis is dependent on *de novo* RNA and protein synthesis (2, 13). However, due to their propensity for rapid apoptosis after a plethora of stimuli, including corticosteroids (14), γ-radiation (15), anti-CD3 antibodies (16), and DNA topoisomerase II inhibitors such as etoposide (VP-16) (9), immature thymocytes have been described as "primed" for apoptotic cell death (4).

The finding that in addition to its physiological role apoptosis can be induced by a diverse array of pathogenic stimuli has led to increased efforts to identify the genes responsible for initiating apoptosis. A number of genes that influence cellular susceptibility to enter apoptosis have been identified, including c-*myc* (17), v-*abl* (18), adenovirus E1A (19), *bcl*-2 (20), and *p53* (21). Wild-type *p53* is classified as a tumor-suppressor gene (22) and has been termed the "guardian of the genome" (23). p53 protein level is stabilized after DNA damage (a post-translational event) and can then induce a G_1 growth arrest (24) and/or direct the induction of apoptosis (25, 26), thus ensuring the prevention of proliferation on a damaged genome. p53 has been proposed to inhibit progression through G_1 into S phase via transactivation of WAF1/Cip1, which inhibits G_1 cyclin-dependent kinases (27, 28), allowing time for DNA repair. The introduction of wild-type p53 into certain cell lines that have lost endogenous p53 function results in growth arrest (29) and/or apoptosis (21, 30). Wild-type p53 but not mutant p53 is required for irradi-

This work was supported in part by the Cancer Research Campaign, UK (CRC Project Grant SP2152/0201) (N.A.J. and C.D.) and the Medical Research Council, UK.

ABBREVIATIONS: bp, base-pair(s); PBS, phosphate-buffered saline; FIGE, field inversion gel electrophoresis; FBS, fetal bovine serum; kbp, kilobase pair(s).

ation-induced apoptosis in thymocytes (31), and p53 exerts a significant and dose-dependent effect on thymocyte apoptosis induced by irradiation and DNA-damaging agents (26). However, these researchers showed that p53-null thymocytes still respond to a number of other apoptotic stimuli, including several that mimic physiological cell deletion signals (i.e., glucocorticoids, calcium-associated activation, and aging *in vitro*).

A recent study from this laboratory to investigate the dependence of thymocyte apoptosis on the phase of the cell cycle demonstrated that glucocorticoids induce apoptosis from G_0/G_1 and G_2/M phases of the cell cycle, whereas etoposide can also induce apoptosis from S phase (32). The majority of immature thymocytes are nonproliferating cells in the G_0 phase of the cell cycle (33). However, using discontinuous Percoll gradient centrifugation, thymocytes can be separated into two distinct subpopulations on the basis of their size: the larger dividing thymocytes obtained constitute 15–20% of total cell number, and the remaining smaller cells are the predominantly quiescent thymocytes (14, 34).

In the current study, we examined the relationship between p53-dependent apoptosis induced by DNA-damaging agents in immature rat thymocytes and their proliferation status. In addition, we asked whether stabilization of p53 by DNA damage correlates directly with subsequent apoptosis. Primary rat thymocytes provide one of the best characterized model systems for the study of apoptosis, as well as a convenient system in which to examine apoptotic death from G_0. Therefore, we separated thymocyte subpopulations by discontinuous Percoll density gradient centrifugation (34) and investigated the sensitivity of two populations comprising proliferatively enriched and predominantly quiescent cells to DNA damage-induced apoptosis. Exposure to DNA-damaging agents induced similar levels of apoptosis in both populations, but only in the former was a marked increase in p53 protein level observed. In contrast, exposure of a purely quiescent population of mature peripheral T cells to DNA-damaging agents resulted in the induction of apoptosis and a concomitant stabilization of p53. These results suggest that DNA-damaging agents can induce apoptosis in a subpopulation of immature thymocytes without an accumulation of p53 and that activation of this pathway is not necessarily dependent on proliferation status but rather on the maturity of the cell population. Furthermore, we demonstrate that DNA-damaging agents can induce a significant level of apoptosis in a subpopulation of immature thymocytes from p53-null mice. These data confirm the presence of an apoptotic pathway in a subpopulation of predominantly quiescent immature thymocytes that can be activated by DNA-damaging agents and is independent of p53.

Materials and Methods

Rat thymocyte preparation and incubations. Male Fischer 344 rats (65–85 g; bred at the University of Leicester) were allowed food and water *ad libitum* and killed with an intraperitoneal overdose of pentobarbitone (Sagatal; 60 mg/kg). Thymocytes were isolated as described previously (35) and diluted with RPMI 1640 (GIBCO BRL, Paisley, Scotland) containing 10% FBS (GIBCO BRL) to give a final suspension of 2×10^7 cells/ml. Unless otherwise stated, incubations were carried out for ≤4 hr at 37° under a humidified atmosphere of 95% air/5% CO_2 in the presence or absence of dexamethasone (0.1 μM) or etoposide (10 μM) or after exposure to γ-radiation (4 Gy). For irradiation, immediately before plating, thymocytes were suspended in 1.5-ml screw-capped nylon tubes and exposed to γ-rays from a Vickrad ^{60}Co source at ~6.5 Gy/min. Where stated, thymocytes were separated by Percoll density gradients into four fractions (F1–F4), as described below. Cells from fractions (F1 or F2) were incubated for ≤4 hr either alone or after exposure to etoposide (10 μM) or γ-radiation (4 Gy).

Peripheral T cell preparation and incubations. Rat mesenteric lymph nodes were isolated from male Fischer 344 rats (130–150 g; bred at the University of Leicester) as described previously (36). Purified peripheral T cells were diluted with RPMI 1640 containing 10% FBS to give a final suspension of 2×10^7 cells/ml. Incubations were carried out for ≤4 hr at 37° under an atmosphere of 95% air/5% CO_2 in the presence or absence of etoposide (10 μM).

Mouse thymocyte incubations. Male p53-null and wild-type mice (4–5 weeks old), generated by the appropriate crosses and genotyped (37), were used to obtain thymocytes as described previously (35). Unless otherwise stated, incubations were carried out for ≤20 hr at 37° under a humidified atmosphere of 95% air/5% CO_2 in the presence or absence of methylprednisolone (10 μM) or etoposide (10 μM) or after exposure to γ-radiation (4 Gy). For irradiation, immediately before plating, thymocytes were resuspended at 1×10^7 cells/ml and exposed to γ-rays from a ^{137}Cs source at 3.8 Gy/min. Where stated, thymocytes were separated by Percoll density gradients, as described below, and cells from fraction F1 or F2 were incubated for ≤4 hr either alone or after exposure to methylprednisolone (10 μM), etoposide (10 μM), or γ-radiation (4 Gy).

Quantification of apoptosis by flow cytometry. Subsequent to treatment, thymocytes or cells from the Percoll fractions were incubated with the bisbenzimidazole dye Hoechst 33342 and propidium iodide to quantify the percentage of apoptotic cells, essentially as described previously (35), except that analysis was performed using a Becton Dickinson FACSVantage flow cytometer and Lysis II software (Becton Dickinson, Oxford, UK). Briefly, 1×10^6 cells were incubated with Hoechst 33342 (1.5 μg/ml) in RPMI 1640 containing 10% FBS at 37° for 10 min. The cells were then cooled to 4°, centrifuged at $200 \times g$ for 5 min, and resuspended in PBS containing propidium iodide (5 μg/ml). Normal thymocytes have a high forward light scatter (indicative of a large size) and exhibit a low blue fluorescence with Hoechst 33342. In contrast, apoptotic cells have a low forward light scatter (indicative of a smaller size) and exhibit a high blue fluorescence. These cells have been shown to be apoptotic based on a number of criteria, including ultrastructure, smaller size, and the presence of DNA ladders (35). In experiments using immature mouse thymocytes, the cells were incubated for ≤20 hr after exposure to an apoptotic agent. Incubation of thymocytes for ≤20 hr results in an increase in the appearance of cells with high blue fluorescence, which over this time period leads to a rise in the proportion of cells that include propidium iodide (secondary necrosis). As a result, the extent of apoptosis in this part of the study was based on the percentage of viable cells (with both low blue fluorescence and propidium iodide exclusion) remaining in the population at each time point.

Percoll gradients. Discontinuous Percoll gradients were used to separate normal and apoptotic thymocytes as described previously (14, 34). The density of the gradients was calibrated by density marker beads. The buoyant densities at the 0–60%, 60–70%, 70–80%, and 80–100% interfaces were 1.063, 1.075, 1.099, and 1.119 g/ml, respectively. Cells were removed from these interfaces (fractions F1–F4, respectively) and mixed with five volumes of RPMI 1640, washed twice, and resuspended in RPMI 1640 containing 10% FBS.

Thymocyte-subset enrichment and phenotyping. Rat thymocytes were isolated as described previously (35) and where stated were separated by Percoll density gradients, as described above, to obtain cell populations F1 and F2. The proliferatively enriched cell population (F1) was then further enriched for $CD4^+CD8^+$ by negative selection with OX-44, a rat homolog of anti-CD53 (38). Cells in

F1 were incubated with saturating monoclonal antibody-containing hybridoma culture supernatant OX-44 (European Collection of Animal Cell Cultures, Salisbury, UK) for 30 min at 4°. The cells were washed twice with ice-cold PBS and then incubated with goat anti-mouse IgG-coated Biomag beads (Advanced Magnetics, Cambridge, MA) at a 10:1 bead-to-cell ratio. The cell suspensions were incubated for 30 min at 4° with gentle mixing every 5 min. Magnetic beads and adhering cells were removed using a magnetic particle separator (model MPC-6, Dynal, Lake Success, NY). The procedure was repeated once again, followed by incubation with goat anti-mouse IgG-coated Dynal beads (Dynal) at a 2:1 bead-to-cell ratio. The cells recovered were enriched from ~75% to >90% for $CD4^+CD8^+$ double-positive cells. Flow cytometric analysis was used to phenotype cell surface markers on total thymocytes, cells in F1 and F2 and cells in F1 obtained after negative selection. Briefly, 2×10^6 cells in PBS containing 0.2% FBS and 0.2% sodium azide were exposed to saturating concentrations of fluorescein isothiocyanate-conjugated anti-CD4 and phycoerythrin-conjugated anti-CD8 (Serotec, Oxford, UK). Analysis was performed on a FACScan flow cytometer (Becton Dickinson) using Lysis II software. Populations of cells expressing markers were calculated from quadrants set using the appropriate negative controls.

DNA analysis. Agarose gel electrophoresis was used to detect DNA laddering in whole cells (2×10^6 cells) according to the method of Sorenson *et al.* (39). DNA of 123 bp or multiples thereof was used as a standard (GIBCO BRL). FIGE was used to resolve large-molecular-weight fragments of DNA. Agarose plugs containing 1×10^6 cells were prepared and analyzed by FIGE as described previously (10). Under the conditions used, DNA fragments ranging in size from 4.4 to 460 kbp were resolved. *Saccharomyces cerevisiae* chromosomes of 243-2200 kbp (Clontech, Cambridge, UK) and DNA of 0.1–200 kbp (Sigma Chemical, Poole, Dorset, UK) were used as standards.

Western blot analysis. Western blot analysis was used to detect p53 protein and Bax protein in rat thymocytes. For each sample, 2×10^7 cells were washed in PBS and lysed in Laemmli buffer (40, 41). The proteins were separated on a 10% SDS-polyacrylamide gel and transferred to supported nitrocellulose (Hybond-C Extra; Amersham International, Buckinghamshire, UK). Electroblotting efficiency and equal protein content per lane were verified by staining of the membranes with 0.1% Ponceau S. Membranes were blocked, and p53 was detected with a specific monoclonal antibody (PAb 421: kindly provided by Prof. D. Lane, University of Dundee, Scotland, UK), which detects both wild-type and mutant p53. The Bax protein was detected using a protein A affinity purified rabbit polyclonal antisera raised against a synthetic peptide of amino acids 44–59 of the murine Bax protein (ELTLEQPPQDASTKKL) (kindly provided by Dr. A. Metcalfe, University of Manchester, Manchester, UK). p53 and Bax were then detected using a horseradish peroxidase-conjugated secondary antibody and a chemiluminescent substrate (ECL; Amersham International). Quantification was performed by densitometric scanning of autoradiographs using a densitometer and ImageQuant software, both from Molecular Dynamics (Sunnyvale, CA).

Results

Etoposide or γ-radiation but not dexamethasone induces p53 in immature rat thymocytes. Incubation of immature rat thymocytes for 4 hr with dexamethasone (0.1 μM) or etoposide (10 μM) or after γ-radiation (4 Gy) resulted in the induction of apoptosis as assessed by both flow cytometry and increased internucleosomal cleavage of DNA to yield a classic DNA ladder (data not shown). As measured by flow cytometry, the percentages of apoptotic cells were 9.6 ± 0.5%, 45.6 ± 7.9%, 31.9 ± 6.0%, and 41.0 ± 6.2% (mean ± standard error; five experiments) in the control and etoposide-, dexamethasone-, and radiation-treated thymocytes, respectively. The flow cytometric method that was used separates and quantifies normal and apoptotic cells, with apoptotic cells exhibiting a decreased cell size and a higher blue fluorescence as a result of increased Hoechst 33342 staining (35, 42). After dexamethasone treatment for 4 hr, no p53 protein was detected by Western blot analysis (Fig. 1). In contrast, cells incubated for 4 hr after exposure to etoposide or radiation exhibited a significant increase in p53 protein levels compared with control cells (Fig. 1). In agreement with previous studies (26, 31), these data demonstrated that p53 expression accompanied apoptosis induced by DNA-damaging agents in thymocytes but apparently was not necessary for glucocorticoid-induced cell death.

Induction of p53 in proliferatively enriched but not quiescent immature rat thymocytes. Given the apparent requirement for p53 accumulation in etoposide- and irradiation-induced apoptosis, we examined the level of p53 protein in two subpopulations of normal immature rat thymocytes that we previously characterized by flow cytometry, gel electrophoresis, and electron microscopy (12, 34). Using Percoll gradient centrifugation, thymocytes were separated into four fractions of decreasing size and increasing density (F1–F4) (34). Based on both ultrastructural and biochemical criteria, the F1 and F2 fractions were enriched for normal proliferatively competent and quiescent thymocytes, respectively (14, 32, 34); cells in F4 were apoptotic, and those in F3 represented a transient population of preapoptotic cells at an early but committed stage of the apoptotic process (12, 34). The cell cycle distribution of unsorted thymocytes and cells in F1 and F2 was verified by flow cytometric analysis: 15% of unsorted cells and 27% of cells in F1 were located in S phase compared with only 4% of cells in F2 (data not shown), confirming that the proliferatively competent cells were enriched in F1. We also confirmed this by using ^{3}H-thymidine incorporation (data not shown).

Freshly isolated thymocytes were separated on Percoll gradients to obtain proliferatively enriched (F1) and primarily quiescent (F2) fractions. These cells were then incubated for ≤4 hr either alone or after exposure to radiation or etoposide. When cells exposed to either agent were analyzed by flow cytometry, apoptotic cells (as assessed by the formation of high blue cells) were clearly detected by 2 hr (Fig. 2). Both etoposide (Fig. 2A) and irradiation (Fig. 2B) caused an equivalent and time-dependent induction of apoptosis in cells from F1 and F2 in comparison with control cells. Degradation of DNA to both large-kilobase-pair and nucleosomal-size fragments is considered an important indicator of biochemical changes associated with apoptosis (11, 12). DNA from both

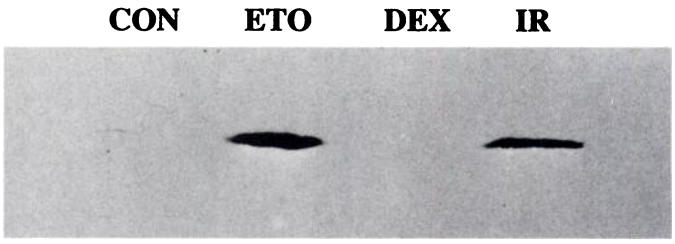

Fig. 1. Detection of p53 levels in immature rat thymocytes after exposure to apoptotic stimuli. Thymocytes were incubated for 4 hr alone (*CON*), after irradiation (*IR*) (4 Gy), or in the presence of etoposide (*ETO*) (10 μM) or dexamethasone (*DEX*) (0.1 μM). Levels of p53 were determined by Western blot analysis of thymocytes obtained 4 hr after exposure to the stimulus.

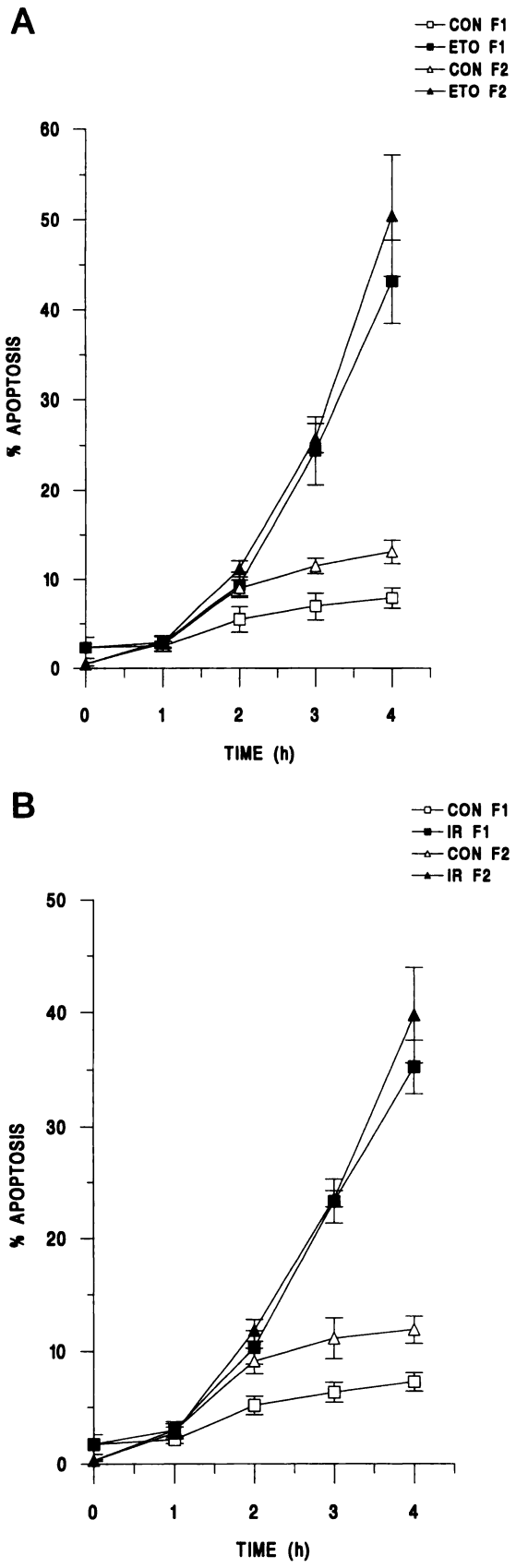

Fig. 2. Detection of apoptosis in proliferatively enriched and quiescent rat thymocytes after exposure to etoposide or radiation. Immature thymocytes were isolated and immediately separated into four subpopulations (F1–F4) as described in Materials and Methods. Proliferatively enriched (*F1*) and quiescent (*F2*) thymocytes, respectively, were then further incubated for ≤4 hr either alone or after exposure to etoposide (*ETO*) (10 μM) (A) or radiation (*IR*) (4 Gy) (B). The level of apoptosis in control (*CON*) (□, ▽) and treated (■, ▼) cells in F1 (□, ■) and F2 (▽, ▼) was assessed by flow cytometry as described in Materials and Methods. Values represent the mean ± standard error from at least three separate experiments.

proliferatively enriched and primarily quiescent thymocytes was examined by both conventional agarose and FIGE. The latter method separates large-kilobase-pair fragments of DNA that subsequently give rise to the DNA ladders characteristic of apoptosis (11, 12). In cells from F1 or F2 incubated for 4 hr without treatment, a small amount of degradation of DNA to large fragments of ~10-50 kbp was observed (*lane 3*, Fig. 3, A and C, respectively). A time-dependent increase in this degradation was observed in cells from F1 and F2 exposed to radiation (*lanes 4–7*, Fig. 3, A and C, respectively) or etoposide (data not shown). On further analysis of these samples by agarose gel electrophoresis, a time-dependent increase in internucleosomal cleavage of DNA was observed (*lanes 4–7*, Fig. 3, B and D). No internucleosomal cleavage was noted at times of ≤2 hr in cells from either F1 (Fig. 3B) or F2 (Fig. 3D), but after this it increased markedly with time in comparison with that observed in control cells (*lane 3*, Fig. 3, B and D).

A marked difference between p53 expression in cells from F1 and F2 was observed after exposure to etoposide (Fig. 4A) or radiation (Fig. 4B). In the proliferatively enriched population (F1), a time-dependent elevation in the level of p53 was detected, with a marked increase first observed after 2 hr of culture (Fig. 4). In contrast, quiescent cells in F2 displayed only a slight increase in p53 by 4 hr (Fig. 4). This small increase in p53 was most likely derived from a minor (~5%) subpopulation of cells from F1 in the F2 fraction. Thus, after exposure to DNA-damaging agents, the proliferatively enriched cells in F1 expressed significantly elevated levels of p53 in comparison with quiescent cells in F2. When thymocytes in F1 or F2 were incubated for 4 hr without treatment, no p53 was detected in either fraction (data not shown). Thus, irradiation and etoposide induced apoptosis to similar levels in both proliferatively enriched (F1) and quiescent (F2) thymocytes (Figs. 2 and 3). However, marked elevations in p53 expression were primarily observed only in the proliferatively enriched cells (Fig. 4).

Induction of apoptosis and accumulation of p53 in quiescent mature rat T cells. The dissociation between induction of apoptosis and accumulation of p53 by DNA-damaging agents in immature quiescent thymocytes (F2) may be a result of either cell cycle status or maturity of the T cells. To distinguish between these possibilities, we obtained a purified population of mature T cells from rat mesenteric lymph nodes. The cell cycle distribution of this population was verified by both flow cytometric analysis and ^{3}H-thymidine incorporation, confirming that ≥98% of the population were quiescent and not cycling. This purified population of mature T cells was then incubated for ≤4 hr either alone or after exposure to etoposide. When assessed by flow cytometry, apoptotic cells were clearly detected by 4 hr; the percentages of apoptotic cells were 10.7 ± 1.9% and 29.3 ± 4.6% (mean ± standard error; four experiments) in the control and etoposide-treated cells, respectively. Quiescent mature T cells incubated for 4 hr with etoposide exhibited a significant

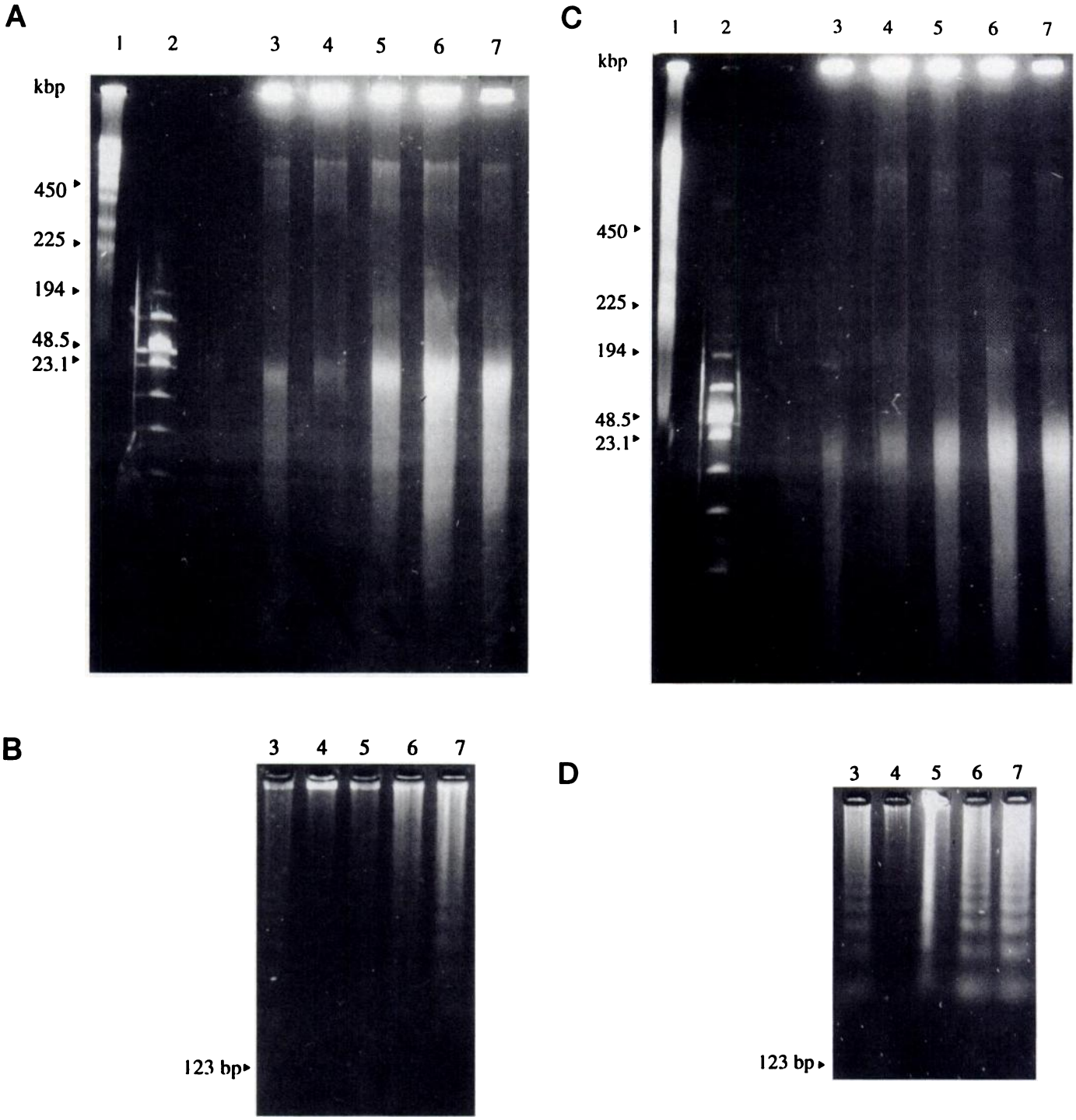

Fig. 3. Determination of the extent of DNA degradation in proliferatively enriched and quiescent thymocytes after irradiation. Thymocytes were isolated and immediately separated into proliferatively enriched (F1) and quiescent (F2) thymocytes. Cells from both fractions were then incubated for ≤4 hr either without treatment or after exposure to radiation (4 Gy). The extent of DNA degradation in cells in F1 (A and B) and F2 (C and D) was determined by both FIGE (A and C) and agarose gel electrophoresis (B and D). *Lane 3*, thymocytes incubated alone for 4 hr. *Lanes 4–7*, cells incubated for 1, 2, 3, or 4 hr, respectively, after exposure to radiation. Standards for FIGE in *lanes 1 and 2* contain 0.1–200 kbp and *S. cerevisiae* chromosomes (243–2200 kbp), respectively, and the distance migrated by several of these size markers is shown. For agarose gel electrophoresis, the distance migrated by the 123-bp standard is indicated.

increase in p53 protein, resulting in a level of protein comparable to that found in our proliferatively enriched thymocyte fraction (F1) at 4 hr (Fig. 5). In agreement with that found previously (Fig. 4A), the predominantly quiescent immature cell fraction (F2) did not show a significant accumulation of p53 protein by 4 hr (Fig. 5). Thus, it was apparent that etoposide induced apoptosis to a similar level in both immature (Fig. 2A) and mature quiescent T cells (see above). However, marked elevations in p53 expression were observed only in mature quiescent T cells (Fig. 5).

DNA-damaging agents can induce apoptosis in immature thymocytes from p53-null mice. Given the ap-

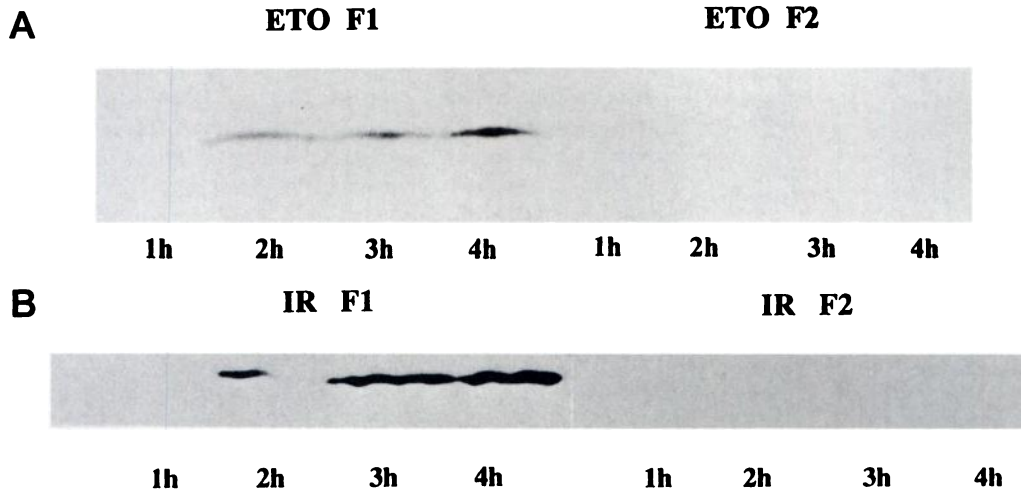

Fig. 4. Determination of p53 levels in proliferatively enriched and quiescent rat thymocytes after exposure to etoposide or radiation. Immature thymocytes were isolated, immediately separated into proliferatively enriched (*F1*) and quiescent (*F2*) cells, and then incubated for 0–4 hr either alone or after exposure to etoposide (*ETO*) (10 μM) (A) or radiation (*IR*) (4 Gy) (B). p53 was detected by Western blot analysis, as described in Materials and Methods, with the treatment of cells indicated above the appropriate lane.

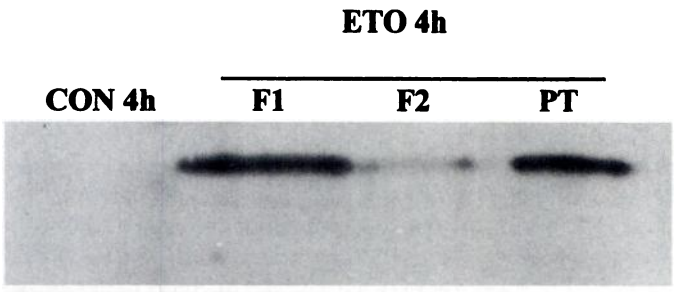

Fig. 5. Comparison of p53 levels in proliferatively enriched and quiescent immature rat thymocytes and quiescent mature T cells. Immature thymocytes were incubated for 4 hr after exposure to etoposide (10 μM) and then separated into proliferatively enriched (*F1*) and quiescent (*F2*) thymocytes. Mature quiescent T cells (*PT*) were purified from rat mesenteric lymph nodes and incubated for ≤4 hr either alone (*CON*) or after exposure to etoposide (*ETO*) (10 μM). Levels of p53 were detected as described in Materials and Methods.

parent dissociation between the level of apoptosis and accumulation of p53 in quiescent immature rat thymocytes (F2), we sought to determine whether unfractionated immature thymocytes (the majority of which are quiescent) can undergo apoptosis in the absence of p53. Immature thymocytes from both wild-type mice and mice carrying a germ-line disruption of the *p53* gene (p53-null) (37) were incubated for ≤20 hr after treatment with the glucocorticoid methylprednisolone (10 μM) or the DNA-damaging agents etoposide (10 μM) or γ-radiation (4 Gy). When cells obtained from wild-type animals were analyzed by flow cytometry, all three agents caused a significant and time-dependent induction of apoptosis in comparison with control cells (Fig. 6A). The extent of apoptosis in these studies was assessed by measuring the percentage of viable cells remaining in the population at each time point (see Materials and Methods). Thymocytes isolated from p53-null animals retained their sensitivity to the glucocorticoid methylprednisolone but were significantly resistant to the induction of apoptosis by the DNA-damaging agents, even ≤20 hr after treatment (Fig. 6B). In agreement with previous studies using unfractionated thymocytes (26, 31), these data demonstrated that p53 is apparently required for the initiation of apoptosis in immature thymocytes but only when it is induced by agents that cause DNA-strand breakage.

To determine whether p53 is required for DNA damage-induced apoptosis after Percoll fractionation of immature mouse thymocytes, we examined the sensitivity of the two subpopulations of proliferatively enriched (F1) and quiescent (F2) cell populations from both wild-type and p53-null mice. Freshly isolated thymocytes were separated on Percoll gradients to obtain F1 and F2 fractions. The cell cycle distribution of unsorted mouse thymocytes and cells in F1 and F2 was verified by flow cytometric analysis: 15% of unsorted cells and 42% of cells in F1 were located in S phase compared with 14% of cells in F2 (data not shown), confirming that the proliferatively competent cells were enriched in F1. Unlike the purified population of quiescent immature rat thymocytes (F2) obtained previously, a pure fraction of quiescent cells in F2 was not obtained through fractionation of mouse thymocytes. Therefore, a comparison of cells in the F2 fractions obtained from rat and mouse cannot be made, at least not on the basis of their cell cycle status.

Cells in F1 and F2 were incubated for ≤20 hr, either alone or after exposure to methylprednisolone, etoposide, or γ-radiation. When cells obtained from wild-type mice were analyzed by flow cytometry, all three agents caused an equivalent induction of apoptosis (as assessed by the percentage of viable cells remaining in the population) in thymocytes from either F1 or F2 when compared with control cells (Fig. 7A). Thymocytes in F1 and F2 that were isolated from p53-null mice retained normal sensitivity to induction of apoptosis by methylprednisolone (Fig. 7B). In contrast, the DNA-damaging agents etoposide and γ-radiation did not induce an equivalent level of apoptosis in fractionated cells obtained from p53-null mice compared with cells from p53 wild-type animals (Fig. 7). However, both etoposide and γ-radiation induced a significant level of apoptosis in cells in F1 and F2 from p53-null mice compared with control cells from p53-null mice (Fig. 7B). In cells in the F1 and F2 Percoll fractions from p53-null mice, γ-radiation induced a significant level (≤20% by 20 hr) of apoptosis (Fig. 7B), and this induction of apoptosis was more evident after exposure to etoposide, with ≤45% of cells being apoptotic by 20 hr (Fig. 7B). This apparent induction of apoptosis by DNA-damaging agents in the absence of p53 was not observed at earlier times of ≤8 hr but was clearly evident by 14 hr (Fig. 7B, *inset*).

To assess whether internucleosomal cleavage of DNA, a classic marker of apoptosis, occurred in parallel with the induction of apoptosis as assessed by flow cytometry, DNA

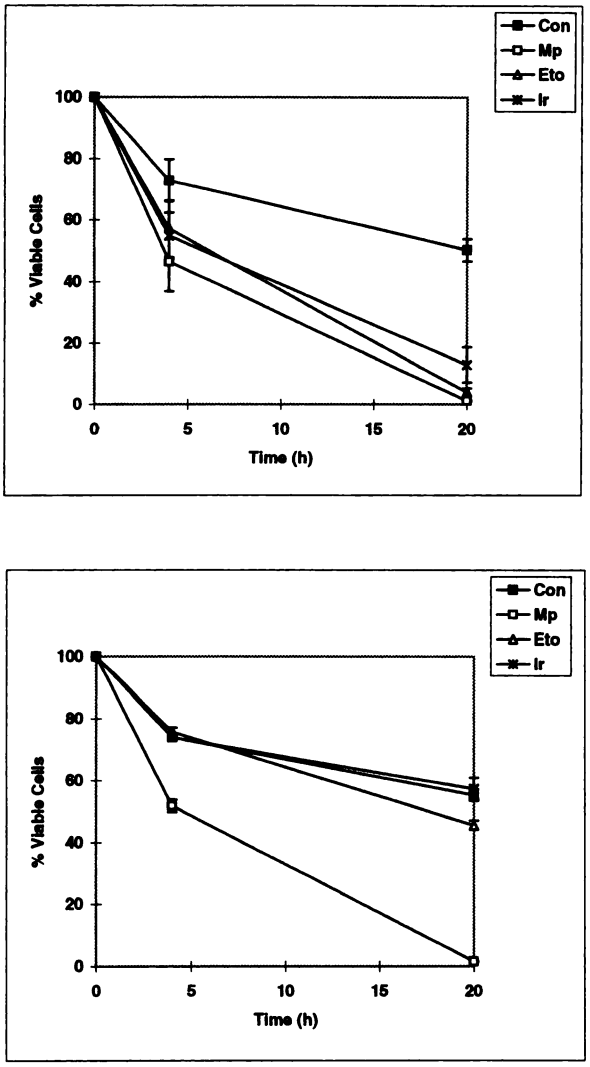

Fig. 6. Detection of apoptosis in immature thymocytes obtained from wild-type and p53-null mice after exposure to apoptotic stimuli. Immature thymocytes were isolated from wild-type and p53-null mice and incubated for ≤20 h either alone (*Con*) (■) or after exposure to methylprednisolone (*Mp*) (10 μM) (□), etoposide (*Eto*) (10 μM) (▽), or γ-radiation (*Ir*) (4 Gy) (*). The level of apoptosis in wild-type (A) and p53-null (B) mice was assessed by flow cytometry as described in Materials and Methods. The percentage of viable cells remaining in the population at 20 hr was used to determine the extent of apoptosis. Values represent the mean ± standard error from three separate experiments. The data were analyzed as a split-plot randomized-block analysis of variance (56).

from either proliferatively enriched (F1) or predominantly quiescent (F2) thymocytes obtained from both wild-type and p53-null mice was examined by conventional agarose gel electrophoresis. An increase in internucleosomal cleavage of DNA was observed in cells in either F1 or F2 from wild-type mice after treatment with all three apoptosis-inducing agents compared with that seen in control cells (data not shown). In the cells from F1 and F2 obtained from p53-null mice, a significant increase in internucleosomal cleavage was observed after treatment with either methylprednisolone or etoposide (Fig. 8). In contrast, γ-radiation resulted in only a small increase in internucleosomal cleavage above that observed in control cells (Fig. 8). Thus, the induction of apoptosis as assessed by the extent of internucleosomal DNA cleavage (Fig. 8) was in agreement with that obtained through the quantitative assessment of apoptosis by flow cytometry (Fig. 7).

Bax levels do not change during DNA damage-induced thymocyte apoptosis. The human *bax* gene is a target for p53-directed transcriptional activation (45). It was therefore of interest to investigate changes in Bax protein levels after DNA damage-mediated stabilization of p53 and the role that Bax may play in the DNA damage-response pathway in mouse thymocytes. As shown in Fig. 9, Bax protein is expressed at a similar level in proliferatively enriched (F1) and predominantly quiescent (F2) thymocytes obtained from both p53 wild-type and p53-null thymocytes. No change in the level of Bax protein could be detected >20 hr after treatment of the p53 wild-type or p53-null thymocytes with the nongenotoxic agent methylprednisolone (Fig. 9) or after exposure to the DNA-damaging agents γ-radiation or etoposide (Fig. 9). Determination of levels of the Bax protein at 4, 8, and 14 hr after the above treatments also showed no change, thus ruling out the possibility that any changes in Bax levels occurred early and transiently after the DNA-damaging insult (data not shown).

DNA damage-induced accumulation of p53 occurs primarily in a subpopulation of CD53-positive thymocytes. Although the majority of immature thymocytes are $CD4^+CD8^+$, the thymus also contains some cells at different stages of development, including immature $CD4^-CD8^-$ and mature $CD4^+CD8^-/CD4^-CD8^+$ cells. Our data demonstrating that accumulation of p53 occurred in parallel with DNA damage-induced apoptosis in quiescent mature T cells (Fig. 5) suggested that stabilization of p53 in thymocytes may be dependent on the maturity of the cell rather than the cell cycle status. We investigated this possibility by determining whether the DNA damage-induced accumulation of p53 observed in immature rat thymocytes may have occurred in a mature subpopulation of cells before their release into the periphery (i.e., in mature single-positive cells). Freshly isolated thymocytes were separated on Percoll gradients to obtain proliferatively enriched (F1) and primarily quiescent (F2) fractions. Cells in F2 comprised primarily immature $CD4^+CD8^+$ double-positive cells (~95%), with only ~4% of cells being either double-negative or single-positive for CD4 or CD8 (Fig. 10A). In contrast, cells in F1 contained only ~75% $CD4^+CD8^+$ cells but were enriched for both immature $CD4^-CD8^-$ and mature $CD4^+CD8^-/CD4^-CD8^+$ cells (~25% in total). Because the majority of p53 detected in thymocytes after DNA damage was observed in cells in F1 (Fig. 4), it was possible that p53 accumulation had occurred predominantly in one of these cell populations for which this fraction was enriched. We investigated this possibility by enriching for immature double-positive cells using negative selection with anti-CD53. Depletion of CD53-expressing cells in F1 resulted in an enrichment for $CD4^+CD8^+$ cells from ~75% to ~93% together with a concomitant loss in single-positive and double-negative cells for CD4 or CD8 (Fig. 10A). Depletion of cells in F1 with anti-CD53 did not significantly alter the percentage of cells in S phase (data not shown). When cells in F1 (before negative selection with anti-CD53) were treated with etoposide, a marked accumulation of p53 was observed (Fig. 10B), which was in agreement with our earlier observations (Fig. 4). In contrast, the identical treatment of cells in F1 after negative selection with anti-CD53 resulted in accu-

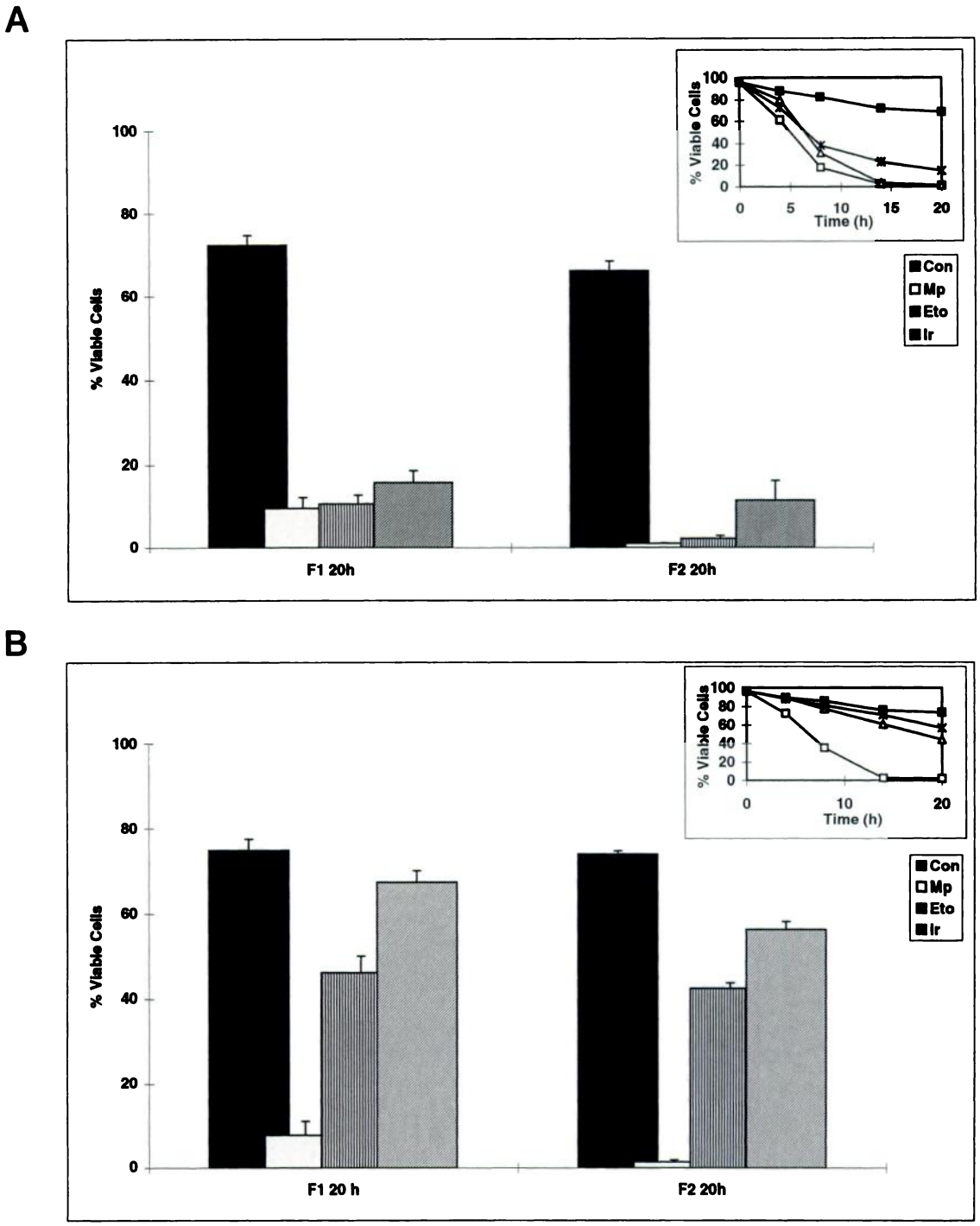

Fig. 7. Detection of apoptosis in immature thymocyte fractions (F1 and F2) obtained from wild-type and p53-null mice. Immature thymocytes were isolated and immediately separated on discontinuous Percoll gradients to obtain a proliferatively enriched fraction (*F1*) and a primarily quiescent fraction (*F2*). Cells from both fractions were then incubated for ≤20 hr either alone (*Con*) or after exposure to methylprednisolone (*Mp*) (10 μM), etoposide (*Eto*) (10 μM), or γ-radiation (*Ir*) (4 Gy). The level of apoptosis in wild-type (A) and p53-null (B) mice was assessed by flow cytometry as described in Materials and Methods. The percentage of viable cells remaining in the population at 20 hr was used to determine the extent of apoptosis. Values represent the mean ± standard error from three separate experiments. *Insets*, time course from a typical experiment for induction of apoptosis in cells in the F2 fraction from wild-type (A) and p53-null (B) mice. Cells were incubated for ≤20 hr either alone (■) or after exposure to methylprednisolone (10 μM) (□), etoposide (10 μM) (▽), or γ-radiation (4 Gy) (*). Differences among groups were compared using Fisher's least significant difference statistic (56).

mulation of only very low levels of p53 (Fig. 10B). Etoposide induced similar levels (~45% by 4 hr) of apoptosis in cells in F1 with or without negative selection. These data demonstrate that the majority of DNA damage-induced p53 accumulation detected in F1 had occurred predominantly in a subpopulation of CD53-positive cells because removal of these cells resulted in a dramatic loss of the p53 response to DNA damage.

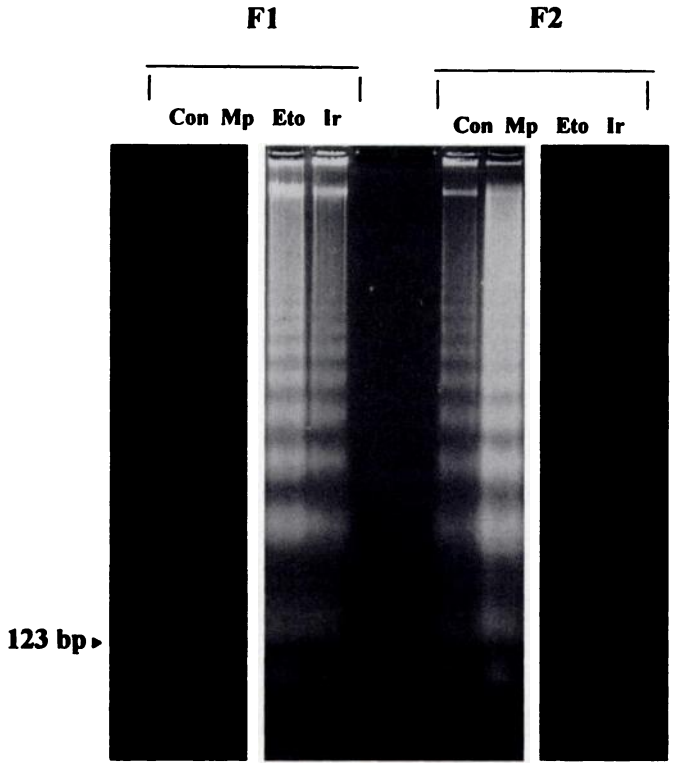

Fig. 8. DNA degradation after exposure to apoptotic stimuli in immature thymocyte fractions obtained from p53-null mice. Immature thymocytes were isolated and immediately separated on discontinuous Percoll gradients to obtain a proliferatively enriched fraction (*F1*) and a primarily quiescent fraction (*F2*). Cells from both fractions were then incubated for 20 hr either alone (*Con*) or after exposure to methylprednisolone (*Mp*) (10 μM), etoposide (*Eto*) (10 μM), or γ-radiation (*Ir*) (4 Gy). The extent of DNA degradation in cells in F1 and F2 was determined by agarose gel electrophoresis as described in Materials and Methods. The distance migrated by the 123-bp standard is indicated.

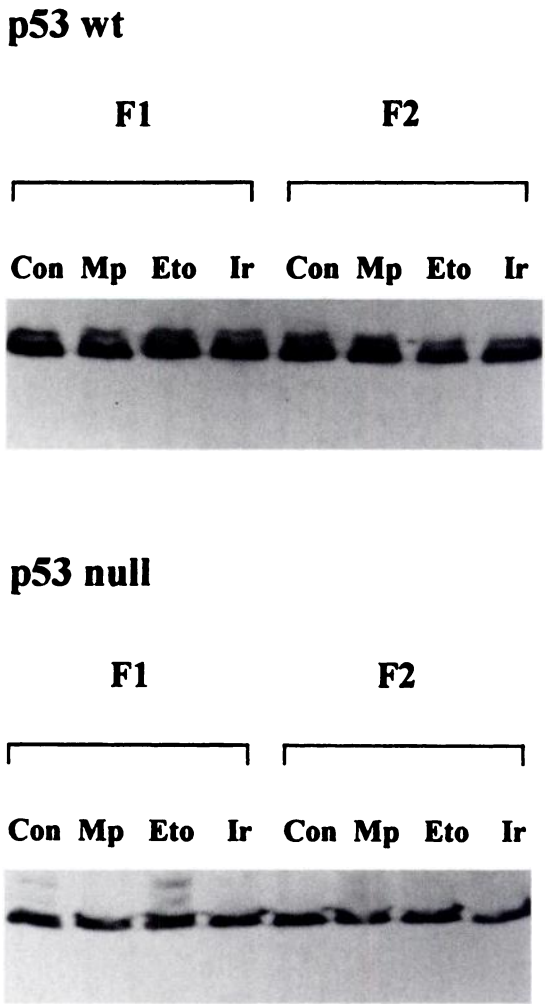

Fig. 9. Determination of Bax protein levels in proliferatively enriched and quiescent p53-null and wild-type mouse thymocytes after exposure to apoptotic stimuli. Immature wild-type and p53-null mouse thymocytes were isolated, immediately separated into proliferatively enriched (*F1*) and quiescent (*F2*) cells, and then incubated for 20 hr either alone (*Con*) or after exposure to methylprednisolone (*Mp*) (10 μM), etoposide (*Eto*) (10 μM), or γ-radiation (*Ir*) (4 Gy). Bax protein was detected by Western blot analysis as described in Materials and Methods. The treatment of cells is indicated above the appropriate lane.

Discussion

DNA-damaging agents induce a p53-independent apoptosis in quiescent immature thymocytes but not in quiescent mature T cells. When thymocytes were enriched for proliferating (F1) and quiescent (F2) cells by Percoll fractionation before the addition of DNA-damaging agents, apoptosis was induced by DNA damage independent of p53 stabilization in the F2 fraction. Percoll fractions F1 and F2 displayed a marked differential sensitivity to stabilization of p53 (Fig. 4) despite being equally susceptible to apoptosis (Figs. 2 and 3). These results suggested that the accumulation of p53 in the proliferatively enriched cell population (F1) either preceded or coincided with the initiation of apoptosis. The very low level of p53 detected in the predominantly quiescent cell fraction (F2) by 4 hr was inconsistent with a critical role for p53 in the onset of apoptosis in quiescent cells. A possibility that cannot be totally excluded is that a very low level of p53, below that detectable by Western blot analysis, is required to induce apoptosis in quiescent immature rat thymocytes. Our data thus suggest that apoptosis may have occurred in these cells via a p53-independent pathway and primarily in a population of quiescent cells.

To investigate whether a p53-independent mechanism persists throughout the development of T cells and correlates with a quiescent state, we measured the accumulation of p53 in mature quiescent T cells isolated from rat mesenteric lymph nodes. After exposure to etoposide, an accumulation of p53 was observed in these cells (Fig. 5) concomitant with the induction of apoptosis. Thus, our observation of an apoptotic pathway induced by DNA-damaging agents and independent of p53 accumulation in quiescent immature thymocytes may be specific to T cells only at a particular stage of development.

Temporal relationship between p53 accumulation and DNA degradation. In addition to a quantitative measurement of apoptosis, the extent of apoptosis induced by DNA damage was assessed by examination of DNA integrity through the use of gel electrophoresis (Fig. 3). That DNA in apoptotic cells (proliferating and quiescent) degrades initially into fragments of >700, 200–300, and 30–50 kbp (10–12) and then to 180-bp integers of the archetypal DNA ladder was confirmed in the current study (Fig. 3). The elevation in p53 observed in proliferatively enriched cells (F1) within 2 hr (Fig. 4) accompanied the formation of large kilobase-pair fragments of DNA (Fig. 3A) and preceded internucleosomal cleavage (Fig. 3B), which is consistent with p53 being re-

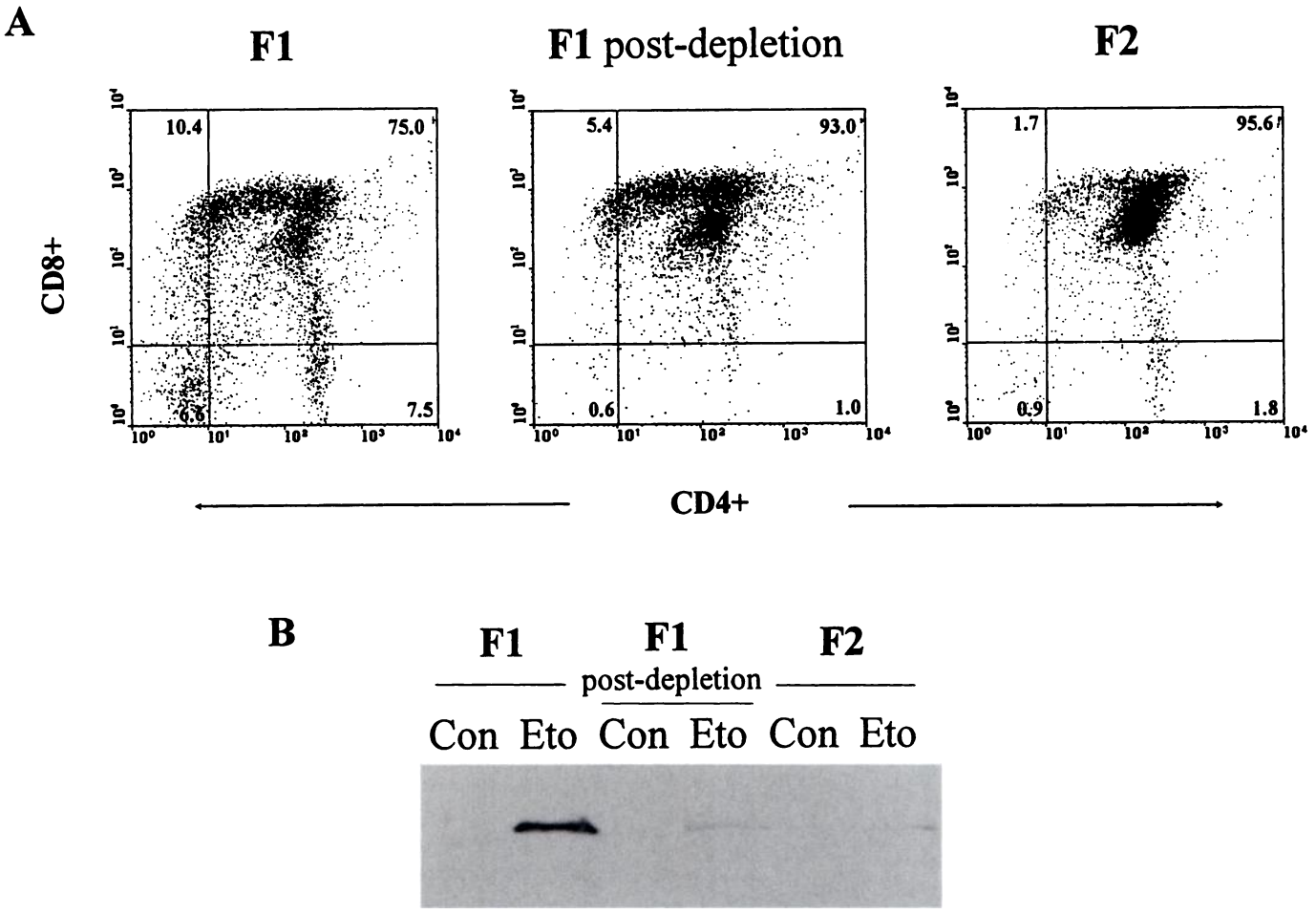

Fig. 10. DNA damage-induced accumulation of p53 in F1 cells is diminished after depletion with anti-CD53. Immature rat thymocytes were isolated and immediately separated into proliferatively enriched (*F1*) and primarily quiescent cells (*F2*). Cells in F1 were further enriched for $CD4^+CD8^+$ by negative selection with anti-CD53. Cells in F1, both before and after depletion, as well as cells in F2 were phenotyped for CD4 and CD8 as described in Materials and Methods. A, The percentage of $CD4^-CD8^-$, $CD4^+CD8^-$, $CD4^-CD8^+$, and $CD4^+CD8^+$ cells are shown in the appropriate quadrants. Cells from F1, both before and after depletion with anti-CD53, and cells in F2 were incubated for 4 hr either alone (*Con*) or with etoposide (*Eto*) (10 μM). B, p53 protein was detected by Western blot analysis as described in Materials and Methods. The treatment of cells is indicated above the appropriate lane.

quired either at the initial cleavage of intact DNA to kilobase-pair fragments or at some stage before their formation. In a population of predominantly quiescent immature thymocytes undergoing apoptosis induced by DNA-damaging agents, a similar increase in the formation of large fragments of DNA was detected within 2 hr (Fig. 3C) but in the absence of any significant elevation in p53 (Fig. 4).

DNA-damaging agents can induce apoptosis in a subpopulation of immature thymocytes from p53-null mice. To rule out the possibility that nondetectable levels of p53 protein could be responsible for DNA damage-induced apoptosis in quiescent immature thymocytes, we examined DNA damage-induced apoptosis in p53-null thymocytes (37). In immature thymocytes (primarily quiescent) obtained from p53-null mice, we identified an apoptotic pathway that was indeed activated by DNA-damaging agents (Figs. 7 and 8). This p53-independent apoptosis was late in onset (20 hr) and less pronounced than the p53-dependent apoptosis observed for p53 wild-type animals (Fig. 7). Interestingly, the DNA topoisomerase II inhibitor etoposide was a much better inducer of apoptosis via this p53-independent pathway than was γ-radiation (Figs. 7 and 8). Thus, it seems that a subpopulation of cells within a primarily quiescent population of immature thymocytes can undergo p53-independent apoptosis in response to DNA-damaging agents. This p53-independent pathway occurs much later and is less sensitive to DNA damage than the major p53-dependent apoptotic pathway in immature thymocytes.

DNA damage-induced accumulation of p53 in T cells is maturation status dependent rather than cell cycle dependent. The ability of DNA-damaging agents to induce apoptosis in p53-null thymocytes was not solely dependent on cell cycle status because cells in both F1 and F2 obtained from p53-null animals were equally susceptible to apoptosis (Figs. 7 and 8). Further characterization of the proliferatively enriched immature thymocyte population F1 revealed that this fraction was also enriched for immature $CD4^-CD8^-$ cells and mature $CD4^+CD8^-/CD4^-CD8^+$ cells (Fig. 10). Enrichment of cells in F1 for $CD4^+CD8^+$ cells by depletion of $CD4^-CD8^-$ and $CD4^+CD8^-/CD4^-CD8^+$ cells with anti-CD53 did not alter their cell cycle status and resulted in very low levels of p53 accumulation induced by DNA damage (Fig. 10). Thus, DNA damage-induced stabilization of p53 in cells in F1 was not cell cycle dependent and had occurred in

immature $CD4^-CD8^-$ cells, mature $CD4^+CD8^-$/$CD4^-CD8^+$ cells, or both. Although we cannot distinguish between these possibilities, it is likely that some of the DNA damage-induced p53 accumulation had occurred in the mature single-positive cells because these are the precursors of mature quiescent peripheral T cells, which also show an accumulation of p53 after treatment with etoposide (Fig. 5). If this is true, then DNA damage-induced accumulation of p53 in thymocytes may be developmentally regulated, as has been reported with other apoptosis-associated genes, such as *bcl*-2 (46).

Bax is not elevated during DNA damage-induced apoptosis. The Bcl-2 family of proteins are important modulators of apoptotic responses to a wide variety of cellular insults in a number of cell types. The Bax protein is a Bcl-2-related protein that can promote cell survival in heterodimeric form with Bcl-2 but can also form homodimers that are thought to precipitate apoptosis and accelerate cell death (47). Of particular interest to the current study is that the human *bax* gene is a target for p53-directed transcriptional activation (45) and could therefore mediate the DNA damage-induced apoptosis via a p53-dependent pathway that we describe. No difference could be detected in the levels of Bax between freshly isolated p53-null cells and their wild-type counterparts. Furthermore, there was no change in the level of Bax protein within thymocytes (wild-type or p53-null) after exposure of these cells to genotoxic stress (see Fig. 9). Increases in the level of *bax* RNA and protein have been shown in M1 myeloid cells expressing a temperature-sensitive mutant of p53 when switched to the permissive temperature (48), and elevation of *bax* RNA occurs after exposure to ionizing irradiation of several cell types that express wild-type p53 (49). *bax* RNA has also been shown to increase on mitogenic stimulation of T cells, a nongenotoxic event, and *bax* RNA levels further increase on irradiation of these cells (50). These data provide further evidence that Bax plays an important role in p53-mediated apoptosis. However, the lack of change in Bax protein levels on induction of apoptosis reported in the current study in p53 wild-type and p53-null thymocytes confirms the previous observation that Bax protein is expressed in the thymus but that this expression has no correlation with areas of the thymus that are undergoing apoptosis (51). In addition, a recent report has also shown that there is no elevation of *bax* RNA on DNA damage-induced elevation of p53 in Burkitt lymphoma and lymphoblastoid cell lines (52). Similarly, Knudson *et al.* (53) reported that Bax-deficient thymocytes display normal sensitivities to γ-radiation, indicating that Bax is not required for p53-dependent apoptosis. These data imply that previous observations that show that Bax plays an important role in p53-mediated apoptosis are cell type dependent (48, 49).

Results of the current study demonstrate that immature thymocytes obtained from p53-null mice undergo apoptosis after exposure to DNA-damaging agents but that this apoptosis occurs in a small subpopulation of cells and is slower in onset than that seen in cells obtained from wild-type animals. The observation that mice homozygous for the null allele of p53 apparently develop normally suggests that p53 is not required for cell death in many, perhaps most, instances during development, although these mice die early from multiple neoplasms (37). The current study is the first demonstration of the induction by DNA-damaging agents of a p53-independent apoptosis in a subpopulation of normal quiescent cells. More evidence for the existence of p53-independent pathways of DNA damage-induced apoptosis has been provided by the study of Strasser *et al.* (54), which demonstrates that mitogenically activated T lymphocytes and cycling T lymphoma cells from p53-null mice can undergo apoptosis after irradiation. Furthermore, recent studies of the induction of apoptosis by γ-radiation in normal intestinal epithelia cells from p53-null mice suggests that DNA damage-induced apoptosis can occur. In agreement with the results presented here for thymocytes, p53-independent apoptosis occurs more slowly within the intestine after irradiation than that seen in the corresponding p53 wild-type cells.[1] Thus, by combining our data with those described above, it becomes apparent that p53-independent pathways of DNA damage-induced apoptosis operate in normal and transformed quiescent and cycling cells.

The mechanism by which DNA damage is sensed by the cell in the absence of p53 is not yet known, although studies of irradiated embryonic fibroblasts that are deficient in interferon regulatory factor-1 suggest that this molecule is a possible candidate (55). The suppression of apoptosis attributable to dysfunctional p53 has been widely reported, and attempts to rectify wild-type p53 function and thus restore apoptotic responses are under way. However, it is becoming increasingly apparent that p53-independent mechanisms of DNA damage-induced apoptosis can operate, and they warrant further investigation.

Acknowledgments

We acknowledge the valuable comments of the referee who raised the possibility of a developmental regulation of p53. We thank Prof. D. Lane for antibody PAb 421, Dr. I. Podmore for operation of the radiation source, and Mr. R. Snowden for help with the flow cytometry. The p53-null and wild-type mice were provided by Prof. C. S. Potten (CRC Paterson Institute, Manchester, UK). We thank David G. Brown and Caroline Chadwick for technical assistance, and we thank Dr. S. Chow (University of Leicester, Leicester, UK) and Dr. R. Brown (Beatson Laboratories, Glasgow, UK) for valuable discussions.

References

1. Kerr, J. F. R., A. H. Wyllie, and A. R. Currie. Apoptosis: a basic biological phenomenon with wide-ranging implications in tissue kinetics. *Br. J. Cancer.* **26**:239–245 (1972).
2. Wyllie, A. H., R. G. Morris, A. L. Smith, and D. Dunlop. Chromatin cleavage in apoptosis: association with condensed chromatin morphology and dependence on macromolecular synthesis. *J. Pathol.* **142**:67–77 (1984).
3. Arends, M. J., R. G. Morris, and A. H. Wyllie. Apoptosis: the role of the endonuclease. *Am. J. Pathol.* **136**:593–608 (1990).
4. Arends, M. J., and A. H. Wyllie. Apoptosis: mechanisms and roles in pathology. *Int. Rev. Exp. Pathol.* **32**:223–254 (1991).
5. Ellis, R. E., J. Yuan, and H. R. Horvitz. Mechanisms and functions of cell death. *Annu. Rev. Cell. Biol.* **7**:663–698 (1991).
6. Cohen, J. J., R. C. Duke, V. A. Fadok, and K. S. Sellins. Apoptosis and programmed cell death in immunity. *Annu. Rev. Immunol.* **10**:267–293 (1992).
7. Wyllie, A. H., J. F. R. Kerr, and A. R. Currie. Cell death: the significance of apoptosis. *Int. Rev. Cytol.* **68**:251–306 (1980).
8. Wyllie, A. H. Glucocorticoid-induced thymocyte apoptosis is associated with endogenous endonuclease activation. *Nature (Lond.)* **284**:555–556 (1980).
9. Walker, P. R., C. Smith, T. Youdale, J. Leblanc, J. F. Whitfield, and M.

[1] A. J. Merrit, C. S. Potten, and J. A. Hickman, submitted for publication.

Sikorska. Topoisomerase II-reactive chemotherapeutic drugs induce apoptosis in thymocytes. *Cancer Res.* **51**:1078–1085 (1991).
10. Brown, D. G., X.-M. Sun, and G. M. Cohen. Dexamethasone-induced apoptosis involves cleavage of DNA to large fragments prior to internucleosomal fragmentation. *J. Biol. Chem.* **268**:3037–3039 (1993).
11. Oberhammer, F., J. W. Wilson, C. Dive, I. D. Morris, J. A. Hickman, A. E. Wakeling, P. R. Walker, and M. Sikorska. Apoptotic death in epithelial cells: cleavage of DNA to 300 and/or 50 kb fragments prior to or in the absence of internucleosomal fragmentation. *EMBO J.* **12**:3679–3684 (1993).
12. Cohen, G. M., X. M. Sun, H. O. Fearnhead, M. MacFarlane, D. G. Brown, R. T. Snowden, and D. Dinsdale. Formation of large molecular weight fragments of DNA is a key committed step of apoptosis in thymocytes. *J. Immunol.* **153**:507–516 (1994).
13. Cohen, J. J., and R. C. Duke. Glucocorticoid activation of a calcium-dependent endonuclease in thymocyte nuclei leads to cell death. *J. Immunol.* **132**:38–42 (1984).
14. Wyllie, A. H., and R. G. Morris. Hormone-induced cell death: purification and properties of thymocytes undergoing apoptosis after glucocorticoid treatment. *Am. J. Pathol.* **109**:78–87 (1982).
15. Sellins, K. S., and J. J. Cohen. Gene induction by γ-irradiation leads to DNA fragmentation in lymphocytes. *J. Immunol.* **39**:3199–3206 (1987).
16. Smith, C. A., G. T. Williams, R. Kingston, E. J. Jenkinson, and J. J. T. Owen. Antibodies to CD3/T-cell receptor complex induce death by apoptosis in immature T cells in thymic cultures. *Nature (Lond.)* **337**:181–184 (1989).
17. Evan, G. I., A. H. Wyllie, C. S. Gilbert, T. D. Littlewood, H. Land, M. Brooks, C. M. Waters, L. Z. Penn, and D. C Hancock. Induction of apoptosis in fibroblasts by c-myc protein. *Cell* **69**:119–128 (1992).
18. Evans, C. A., P. J. Owen-Lynch, A. D. Whetton, and C. Dive. Activation of the Abelson tyrosine kinase activity is associated with suppression of apoptosis in hemopoietic cells. *Cancer Res.* **53**:1735–1738 (1993).
19. Rao, L., M. Debbas, P. Sabbatini, D. Hockenbery, S. Korsmeyer, and E. White. The adenovirus E1A proteins induce apoptosis, which is inhibited by the E1B 19-kDa and Bcl-2 proteins. *Proc. Natl. Acad. Sci. USA* **89**: 7742–7746 (1992).
20. Hockenbery, D., G. Nuñez, C. Milliman, R. D. Schreiber, and S. J. Korsmeyer. Bcl-2 is an inner mitochondrial membrane protein that blocks programmed cell death. *Nature (Lond.)* **348**:334–336 (1990).
21. Yonish-Rouach, E., D. Resnitzky, J. Lotem, L. Sachs, A. Kimchi, and M. Oren. Wild-type p53 induces apoptosis of myeloid leukaemic cells that is inhibited by interleukin-6. *Nature (Lond.)* **352**:345–347 (1991).
22. Finlay, C. A., P. W. Hinds, and A. J. Levine. The p53 proto-oncogene can act as a suppressor of transformation. *Cell* **57**:1083–1093 (1989).
23. Lane, D. P. A death in the life of p53. *Nature (Lond.)* **358**:15–16 (1992).
24. Kastan, M. B., O. Onyekwere, D. Sidransky, B. Vogelstein, and R. W. Craig. Participation of p53 protein in the cellular response to DNA damage. *Cancer Res.* **51**:6304–6311 (1991).
25. Lowe, S. W., H. E. Ruley, T. Jacks, and D. E. Housman. p53-Dependent apoptosis modulates the cytotoxicity of anticancer agents. *Cell* **74**:957–967 (1993).
26. Clarke, A. R., C. A. Purdie, D. J. Harrison, R. G. Morris, C. C. Bird, M. L. Hooper, and A. H. Wyllie. Thymocyte apoptosis induced by p53-dependent and independent pathways. *Nature (Lond.)* **362**:849–852 (1993).
27. Harper, J. W., G. M. Adami, N. Wei, K. Keyomarsi, and S. J. Elledge. The p21 Cdk-interacting protein Cip1 is a potent inhibitor of G1 cyclin-dependent kinases. *Cell* **75**:805–816 (1993).
28. El-Deiry, W. S., J. W. Harper, P. M. O'Connor, V. E. Velculescu, C. E. Canman, J. Jackman, J. A. Pietenpol, M. Burrell, D. E. Hill, Y. Wang, K. G. Wiman, W. E. Mercer, M. B. Kastan, K. W. Kohn, S. J. Elledge, K. W. Kinzler, and B. Vogelstein. *WAF1/CIP1* is induced in *p53*-mediated G_1 arrest and apoptosis. *Cancer Res.* **54**:1169–1174 (1994).
29. Baker, S. J., S. Markowitz, E. R. Fearon, J. K. V. Wilson, and B. Vogelstein. Suppression of human colorectal carcinoma cell growth by wild-type p53. *Science (Washington D. C.)* **249**:912–915 (1990).
30. Shaw, P., R. Bovey, S. Tardy, R. Sahli, B. Sordat, and J. Costa. Induction of apoptosis by wild-type p53 in a human colon tumor-derived cell line. *Proc. Natl. Acad. Sci. USA* **89**:4495–4499 (1992).
31. Lowe, S. W., E. M. Schmitt, S. W. Smith, B. A. Osborne, and T. Jacks. p53 is required for radiation-induced apoptosis in mouse thymocytes. *Nature (Lond.)* **362**:847–849 (1993).
32. Fearnhead, H. O., M. Chwalinski, R. T. Snowden, M. G. Ormerod, and G. M. Cohen. Dexamethasone and etoposide induce apoptosis in rat thymocytes from different phases of the cell cycle. *Biochem. Pharmacol.* **48**:1073–1079 (1994).
33. Bruno, S., P. Lassota, W. Giaretti, and Z. Darzynkiewicz. Apoptosis of rat thymocytes triggered by prednisolone, camptothecin, or teniposide is selective to G_0 cells and is prevented by inhibitors of proteases. *Oncol. Res.* **4**:29–35 (1992).
34. Cohen, G. M., X.-M. Sun, R. T. Snowden, M. G. Ormerod, and D. Dinsdale. Identification of a transitional preapoptotic population of thymocytes. *J. Immunol.* **151**:566574 (1993).
35. Sun, X.-M., R. T. Snowden, D. N. Skilleter, D. Dinsdale, M. G. Ormerod, and G. M. Cohen. A flow cytometric method for the separation and quantitation of normal and apoptotic thymocytes. *Anal. Biochem.* **204**:351–356 (1992).
36. Hudson L., and F. C. Hay. *Practical Immunology*. Blackwell Scientific Publications, London (1980).
37. Kemp, C. J., L. A. Donehower, A. Bradley, and A. Balmain. Reduction of p53 gene dosage does not increase initiation or promotion but enhances malignant progression of chemically induced skin tumours. *Cell* **74**:813–822 (1993).
38. Paterson, D. J., J. R. Green, W. A. Jefferies, M. Puklavec, and A. F. Williams. The MRC OX-44 antigen marks a functionally relevant subset among rat thymocytes. *J. Exp. Med.* **165**:1–13 (1987).
39. Sorenson, C. M., M. A. Barry, and A. Eastman. Analysis of events associated with cell cycle arrest at G2 phase and cell death induced by cisplatin. *J. Natl. Cancer Inst.* **82**:749–755 (1990).
40. Harlow, E., and D. Lane. *Antibodies: A Laboratory Manual*. Cold Spring Harbor Press, Cold Spring Harbor, NY (1988).
41. Laemmli, U. K. Cleavage of structural proteins during the assembly of the head of bacteriophage T4. *Nature (Lond.)* **227**:680–685 (1970).
42. Ormerod, M. G., X.-M. Sun, R. T. Snowden, R. Davies, H. Fearnhead, and G. M. Cohen. Increased membrane permeability of apoptotic thymocytes: a flow cytometric study. *Cytometry* **14**:595–602 (1993).
43. Ullrich, S. J., W. E. Mercer, and E. Appella. Human wild-type p53 adopts a unique conformational and phosphorylation state *in vivo* during growth arrest of glioblastoma cells. *Oncogene* **7**:1635–1643 (1992).
44. Gannon, J. V., R. Greaves, R. Iggo, and D. Lane. Activating mutations in p53 produce a common conformational effect: a monoclonal antibody specific for the mutant form. *EMBO J.* **9**:1595–1602 (1990).
45. Miyashita, T., and J. C Reed. Tumour suppressor p53 is a direct transcriptional activator of the human *bax* gene. *Cell* **80**:293–299 (1995).
46. Veis, D. J., C. L. Sentman, E. A. Bach, and S. J. Korsmeyer. Expression of the Bcl-2 protein in murine and human thymocytes and in peripheral T lymphocytes. *J. Immunol.* **151**:2546–2554 (1993).
47. Oltvai, Z. N., C. L. Milliman, and S. J. Korsmeyer. Bcl-2 heterodimerizes in vivo with a conserved homolog, Bax, that accelerates programmed cell death. *Cell* **74**:609–619 (1993).
48. Selvakumaran, M., H.-S. Lin, T. Miyashita, H. G. Wang, S. Krajewski, J. C. Reed, B. Hoffman, and D. Liebermann. Immediate up-regulation of *bax* expression by p53 but not TGF 66 1: a paradigm for distinct apoptotic pathways. *Oncogene* **9**:1791–1798 (1994).
49. Zhan, Q., S. Fan, I. Bae, C. Guillof, D. A. Liebermann, P. M. O'Connor, and A. J. Fornace, Jr. Induction of *bax* by genotoxic stress in human cells correlates with normal p53 status. *Oncogene* **9**:3743–3751 (1994).
50. Tamura, T., M. Ishihara, M. S. Lamphier, N. Tanaka, I. Oishi, S. Aizawa, T. Matsuyama, T. W. Mak, S. Taki, and T. Tanaguchi. An IRF-1-dependent pathway of DNA damage-induced apoptosis in mitogen-activated T lymphocytes. *Nature (Lond.)* **376**:596–599 (1995).
51. Krajewski, S., M. Krajewski, A., Shabaik, T. Miyashita, H. G. Wang, and J. C. Reed. Immunohistochemical determination of *in vivo* distribution of Bax, a dominant inhibitor of Bcl-2. *Am. J. Pathol.* **145**:1323–1336 (1994).
52. Allday, M. J., A. Sinclair, G. Parker, D. H. Crawford, and P. J. Farrell. Epstein-Barr virus immortalizes human B cells without neutralizing the functions the function of p53. *EMBO. J.* **14**:1382–1391 (1995).
53. Knudson, C. M., K. S. K. Tung, W. G. Tourtellotte, G. A. J. Brown, and S. J. Korsmeyer. Bax-deficient mice with lymphoid hyperplasia and male germ cell death. *Science (Washington D. C.)* **270**:96–98 (1995).
54. Strasser, A., A. W. Harris, T. Jacks, and S. Cory. DNA damage can induce apoptosis in proliferating lymphoid cells via p53-independent mechanisms inhibitable by Bcl-2. *Cell* **79**:329–339 (1994).
55. Tanaka, N., M. Ishihara, M. Kitagawa, H. Harada, T. Kimura, T. Matsuyama, M. S. Lamphier, S. Aizawa, T. W. Mak, and T. Taniguchi. Cellular commitment to oncogene-induced transformation or apoptosis is dependent on the transcription factor IRF-1. *Cell* **77**:829–839 (1994).
56. Snedecor, G. W., and W. G. Cochran. *Statistical Methods*. Iowa State University Press, Ames (1980).

Send reprint requests to: Dr. Marion MacFarlane, MRC Toxicology Unit, Hodgkin Building, University of Lancaster, P.O. Box 138, Lancaster Road, Leicester LE1 9HN, United Kingdom. E-mail: mm21@leic.ac.uk